Journal of Catalysis 301 (2013) 116–124

Contents lists available at SciVerse ScienceDirect

Journal of Catalysis

journal homepage: www.elsevier.com/locate/jcat

# Reaction pathways over copper and cerium oxide catalysts for direct synthesis of imines from amines under aerobic conditions

Linda Al-Hmoud, Christopher W. Jones *

*School of Chemical & Biomolecular Engineering, Georgia Institute of Technology, 311 Ferst Dr., Atlanta, GA 30332-0100, United States*

ARTICLE INFO

*Article history:*
Received 20 September 2012
Revised 26 January 2013
Accepted 28 January 2013

*Keywords:*
CuO
$CeO_2$
Mixed oxide
Oxidation
Catalyst
Oxidative coupling
Oxidative dehydrogenation
Leaching

ABSTRACT

Copper(II) oxide, cerium oxide, and several copper(II) oxide supported on cerium oxide catalysts are explored in the aerobic oxidative homocoupling of benzylamine to form N-benzylidenebenzylamine in DMSO at 110 °C. Although both CuO and $CeO_2$ alone are shown to catalyze the reaction, CuO—$CeO_2$ catalysts are shown to most efficiently catalyze the reaction, providing higher rates (per g Cu) due to the presence of both copper and ceria species in the reactor. Catalysts with lower copper loadings and increased ceria content reduce the product yield, as ceria domains can catalyze the decomposition of the desired product as well. The amine conversion occurs with a significant induction period, associated with the putative formation of an initial benzylimine intermediate in the case of catalysis with $CeO_2$ alone or from slow copper solubilization in cases where supported or unsupported copper catalysts are used, followed by rapid conversion to the N-benzylidenebenzylamine product. Copper leaching studies clearly demonstrate that catalysis using copper-containing catalysts is primarily associated with turnover by soluble copper species. A series of experiments targeted at elucidating the reaction pathway suggests that copper oxide domains promote the coupling of the initial intermediate, benzylimine, with benzylamine to produce the N-benzylidenebenzylamine product (path A), with a maximum production rate of 888 μmol/$m^2$ h (13.3 mmol/gCu h) over the pure CuO catalyst or 22.9 μmol/$m^2$ h (26.1 mmol/gCu h) over the CuO—$CeO_2$ catalyst. In contrast, cerium oxide domains are suggested to primarily convert the benzylimine to benzaldehyde, followed by condensation of the benzaldehyde with benzylamine in a rapid step to yield the N-benzylidenebenzylamine product (path B), with a maximum amine production rate of 2.74 μmol/$m^2$ h. Both ceria and copper(II) oxide domains promote the initial benzylimine formation at comparable rates. Although the CuO—$CeO_2$ catalyst leaches about 11% of the copper during the reaction, and these soluble copper species are largely responsible for the catalytic turnover, the recovered solid can be recycled until the copper is depleted, catalyzing the reaction with an identical rate per g Cu in a second cycle, after calcination. The copper–ceria family of catalysts offers an alternative, potentially lower cost composition for the target oxidative homocoupling reaction than previously studied precious metal catalysts, although copper leaching is a distinct drawback to the catalyst composition.



## 1. Introduction

Imines are important intermediates in the synthesis of various biologically active nitrogen-containing compounds. Imines are traditionally synthesized by several methods, including direct synthesis from amines and alcohols in the presence of catalyst and base [1–8], self-condensation of primary amines with oxidants [6,9–14], and via oxidation of secondary amines [12,15–20]. In the last several years, it has been demonstrated that imines can be synthesized by conversion of two moles of the parent primary amine under oxidative conditions in the presence of a variety of suitable catalysts [6,9,10,12,13,15,18,21–33]. A prototypical reaction of this type is benzylamine oxidative homocoupling to form N-benzylidenebenzylamine. This reaction has been reported to be catalyzed by homogeneous copper(I) chloride under mild aerobic conditions [13], a copper(II) complex [31], bulk gold powder [18] and supported gold nanoparticles [27,32,34], ruthenium N-heterocyclic carbene (NHC) catalysts [21], $V_2O_5$ catalysts with aqueous hydrogen peroxide [9], and by a molecular vanadium complex catalyst, $VO(Hhpic)_2$ [33] among others.

Copper oxide supported on ceria (CuO—$CeO_2$) is known to be a highly effective catalyst in NO reduction [35–46], CO and hydrocarbon oxidations [37,46–49], the water–gas shift reaction [50–54], and in many other reactions. This catalytic reactivity is generally ascribed to the synergistic interactions of CuO and $CeO_2$, which are related to their interdispersivity, the facile creation of defects (e.g., oxygen vacancies), and redox interplay between copper and

* Corresponding author. Fax: +1 404 894 2866.
*E-mail address:* cjones@chbe.gatech.edu (C.W. Jones).

0021-9517/$ - see front matter © 2013 Elsevier Inc. All rights reserved.
http://dx.doi.org/10.1016/j.jcat.2013.01.027

cerium redox couples ($Cu^{2+}/Cu^{+}$ and $Ce^{4+}/Ce^{3+}$) [55,56]. While exploring CuO—$CeO_2$ catalysts for other reactions, we serendipitously discovered it to be highly efficient in the aerobic oxidation of benzylamine to form N-benzylidenebenzylamine. Following this initial observation, we carried out a systematic study of the conversion of benzylamine in the title reaction, establishing the role of the copper species and ceria support on the reaction.

## 2. Experimental

### 2.1. Catalyst preparation

A commercial mesoporous $CeO_2$ (Rhodia, $S_{BET}$ = 211 $m^2/g$, average pore diameter = 3.2 nm, pore volume = 0.130 $cm^3/g$, 4–5 μm particle diameter) was used as received. The CuO—$CeO_2$ catalyst was prepared by wetness impregnation. First, 5 g of $CeO_2$ was added to 0.75 ml of 2.57 g/ml aqueous solution of $Cu(NO_3)_2{\cdot}3H_2O$ (Sigma–Aldrich, purity >99%) as a precursor, to yield a 9 wt% ceria-supported copper catalyst. Then, the catalyst was heated to 120 °C at ramp of 3 °C/min in an air flow and dried at 120 °C for 3 h. Then, it was further heated to 500 °C at ramp of 3 °C/min and calcined in flowing air at 500 °C for another 3 h. Elemental analysis established the copper content in this CuO—$CeO_2$ catalyst as 9.2 wt%, and thus, it is referred to as CeCu(II)09. Two additional catalysts with lower copper oxide loadings were prepared similarly, CeCu(II)01 and CeCu(II)05, using the appropriate $Cu(NO_3)_2{\cdot}3H_2O$ concentration to yield 1 wt% and 5 wt% copper, respectively.

Commercial CuO nanoparticles (Sigma–Aldrich, $S_{BET}$ = 12 $m^2/g$) were used as received for comparison purposes.

### 2.2. Characterization

Powder X-ray diffraction (PXRD) was carried out with a PAnalytical X'Pert PRO diffractometer operating with Cu Kα radiation and an X'celerator RTMS detector. A step size of 0.002° 2θ and a scan rate of 10 s per step were used. Nitrogen-adsorption isotherms were recorded at 77 K using a Micromeritics TriStar II 3020. BET (Brunauer–Emmett–Teller) surface areas were calculated using adsorption data. Average pore diameters were determined by BDB–FHH method (a simplified Broekhoff–de Boer method with a Frenkell–Halsey–Hill isotherm)[57]. Elemental analysis by ICP-AES was carried out by Columbia Analytics (Tucson, AZ). Scanning electron microscopy (SEM) images and electron-dispersive X-ray (EDX) analysis were obtained on a JEOL LEO-1530 at a landing energy of 15 kV using the "In Lens" mode detector. Hydrogen-temperature programmed reduction ($H_2$-TPR) was measured using approximately 150 mg of fresh catalysts in a Micromeritics AutoChem II 2920. The samples were placed in a U-shaped tube and first oxidized in 10%$O_2$–He flow of 60 ml/min while heating from room temperature to 600 °C at 10 °C/min, then passivated under helium and returned to room temperature. The TPR spectra were then recorded by heating the samples from room temperature to 400 °C at 10 °C/min, under 60 ml/min flow of 10% $H_2$–Ar mixture.

### 2.3. Catalytic conversion of benzylamine to N-benzylidenebenzylamine

The catalyst, generically coded as CeCu(X)YY (0.05 eq. Cu relative to the amine), was added to a 25-ml two-neck round bottom flask containing 3 mmol benzylamine (327 μl), 3 ml DMSO, and 1.5 mmol diphenyl ether (0.5 eq., 238 μl) as an internal standard. The round bottom flask was attached to a condenser and immersed in a preheated oil bath, at 110 °C, in an air atmosphere, to start the reaction. Samples of the reaction mixture were taken by a needle and a syringe through a rubber septum at specified times, filtered over silica gel column, and diluted with ethyl acetate, and the product yield was determined by GC–FID. The identity of the product was verified by GC–MS. The product yield is calculated by dividing the product concentration by the initial concentration of the reactant, benzylamine, after calibrating the GC–FID peak in reference to the internal standard, diphenyl ether.

## 3. Results and discussion

### 3.1. Catalyst characterization

Table 1 shows the copper and cerium content of the synthesized catalysts. The results are close to the theoretical values. PXRD patterns for the catalysts are shown in Fig. S1. Using these patterns and the Scherrer equation, the crystallite sizes of the copper and cerium domains are estimated and listed in Table 1. The PXRD patterns of CeCu(II)01 and CeCu(II)05 (not shown) are very similar to that of pure mesoporous $CeO_2$, with no detectable crystalline CuO peaks (e.g., at 2θ = 35.7° and 38.8°), suggesting high dispersion of CuO on the ceria support.

Crystalline CuO peaks are clearly detected in the CeCu(II)09 material, and the crystallite size of the largest particles was estimated using the Scherrer equation to be 28 nm, as shown in Table 1. Knowing that the mesoporous $CeO_2$ average pore diameter was around 4 nm, based on the nitrogen physisorption isotherms (see below), and that the support particle size is 4–5 μm, Fig. S2, it appears that the large, crystalline CuO domains were on the outer surface of $CeO_2$ crystallites, but may be also contained within the $CeO_2$ particles. In addition, there were some unsupported CuO particles observed in TEM images (not shown), which were estimated by $H_2$-TPR (below) to represent 35% of the total CuO present in the sample.

The porosity of the $CeO_2$ was characterized using nitrogen physisorption at 77 K. The material had a relatively high BET surface

**Table 1**
Physical properties of the composite Cu/$CeO_2$ catalysts, CuO nanoparticles, and $CeO_2$ support.

| Catalyst | Cu (wt%) | Cu/Ce (mol/mol) | $S_{BET}$ ($m^2/g$) | Micropore area[a] ($m^2/g$) | Average pore diameter(s)[a] (nm) | Cumulative pore volume[a] ($cm^3/g$) | [Cu] Crystallite size[b] (nm) | [Ce] Crystallite size[c] (nm) |
|---|---|---|---|---|---|---|---|---|
| $CeO_2$ | – | – | 211 | 11 | 2.6, 4.5 | 0.130 | – | 5.0 |
| Calcined[d]-$CeO_2$ | – | – | 153 | 7 | 4.0 | 0.161 | – | 6.0 |
| CuO | – | – | 12 | | – | – | 19 | – |
| CeCu(II)01 | 1.1 | 0.031 | 127 | 8 | 3.6, 5.0 | 0.141 | – | 6.5 |
| CeCu(II)05 | 5.3 | 0.153 | 105 | 13 | 3.4, 5.3 | 0.114 | – | 6.7 |
| CeCu(II)09 | 9.2 | 0.269 | 105 | 4 | 3.7, 7.3 | 0.120 | 28 | 6.1 |

[a] Calculated from nitrogen-adsorption isotherms at 77 K, using *t*-plot for micropore area, and BDB–FHH method for average pore diameter and cumulative pore volume.
[b] Estimated using the Scherrer equation, from X-ray line-broadening at 2θ = 35.5°.
[c] Estimated using the Scherrer equation, from X-ray line-broadening at 2θ = 28.5°.
[d] After calcination at 500 °C.

**Table 2**
$H_2$-TPR analysis results of for three supported CuO catalysts, CeCu(II)01, CeCu(II)05, CeCu(II)09, and CuO nanoparticles.

| CeCu(II)01 | | CeCu(II)05 | | CeCu(II)09 | | CuO nanoparticles | |
|---|---|---|---|---|---|---|---|
| *T* (°C) | $H_2$ consumption (μmol/g) | *T* (°C) | $H_2$ consumption (μmol/g) | *T* (°C) | $H_2$ consumption (μmol/g) | *T* (°C) | $H_2$ consumption (μmol/g) |
| 159 | 190 | 86 | 490 | 76 | 650 | 185 | 2723 |
| 217 | 240 | 95 | 360 | 105 | 240 | 229 | 7170 |
| 288 | 210 | 110 | 300 | 128 | 540 | | |
| | | 129 | 190 | 140 | 460 | | |
| Total | 640 | Total | 1340 | Total | 1890 | Total | 9893 |
| Theoretical | 167 | Theoretical | 836 | Theoretical | 1454 | Theoretical | 12,572 |
| Reduction in $CeO_2$ | 473 (74% of $H_2$) | Reduction in $CeO_2$ | 504 (38% of $H_2$) | Reduction in $CeO_2$ | 436 (23% of $H_2$) | | |

area, 211 $m^2$/g, which decreased to 153 $m^2$/g upon calcination at 500 °C. The average pore diameter and the cumulative pore volume of the as received mesoporous $CeO_2$ were 3.2 nm and 0.13 $cm^3$/g, respectively, and they changed to 4.0 nm and 0.16 $cm^3$/g upon calcination. The crystallite size of $CeO_2$ also increased from 5.0 nm to 6.0 nm after calcination. Fig. S3 shows the pore size distribution of the ceria support and the synthesized catalysts. It can be noted that upon calcination of the $CeO_2$, the pore size distribution changed from bimodal with 2.6 and 4.5 nm average pore diameters to a mono-modal distribution with 4.0 nm average pore diameter. The pore diameter of 3.8 nm was unchanged upon incorporation of copper onto the solid.

Supporting CuO on $CeO_2$ and progressively increasing the CuO loading reduced the BET surface area and changed the pore size distribution from mono-modal to bimodal. This may suggest that copper oxide interacts with $CeO_2$ particles in such a way as to create the new, larger pores seen in the pore size distribution curves in the range from 5 to 8 nm (Fig. S3). Nonetheless, these pore size changes are subtle, and significant changes in porosity upon copper addition are not evident.

Table 2 and Fig. S4 show and summarize $H_2$-TPR patterns for the three supported CuO—$CeO_2$ catalysts, specifically CeCu(II)01, CeCu(II)05, CeCu(II)09, bare $CeO_2$, and for unsupported CuO nanoparticles, as a reference. It is known that $CeO_2$ has two reduction peaks at about 430 °C and 900 °C, which are ascribed to the reduction in surface and bulk oxygen of $CeO_2$, respectively [58]. Although bulk CuO has been shown to reduce at 300–400 °C [59–61], the $H_2$-TPR pattern of unsupported CuO nanoparticles shown in Fig. S4 starts reduction at a much lower temperature, 100 °C, and has one main peak at 229 °C, with a leading shoulder at 185 °C. This lower reduction temperature may be associated with the nanoparticle nature of the CuO sample, as it has been shown that when the particle size of CuO was decreased, the materials are more easily reduced [62]. Also, it has been shown in the literature that the shape and position of the $H_2$-TPR peaks of CuO—$CeO_2$ system depend on the copper content, the type of copper species, the interaction between CuO and $CeO_2$, and on the surface area of the support [59–61,63,64]. The CeCu(II)01 material contained minimal reducible material, as expected from the low CuO loading, and showed a broad peak centered at 159 °C and another weaker broad peak at 288 °C. The total $H_2$ consumption was 640 μmol/g. Theoretically, for a 1 wt% Cu sample, 167 μmol $H_2$/g was required to completely reduce all the CuO to metallic copper. The difference, 473 μmol $H_2$/g, was expected to be associated with reduction in the ceria support. Since the CuO in CeCu(II)01 was highly dispersed, as indicated by PXRD, the $H_2$-TPR reduction peak at 159 °C can be related to highly dispersed CuO particles and/or $Cu^{2+}$ isolated species, while the high temperature peaks, 217 °C and 288 °C, may be associated with the reduction in surface ceria [59–61].

The reduction profile for the CeCu(II)05 material included a sharp peak at 86 °C with a shoulder at 95 °C and another smaller peak at 129 °C, with a total $H_2$ consumption of 1340 μmol $H_2$/g. As suggested by Ayastuy [61], the former peak may be related to reduction in highly dispersed CuO domains that are not strongly interacting with the $CeO_2$ support, whereas the latter peak was likely associated with the simultaneous reduction in ceria and the CuO species that were directly interacting with $CeO_2$ support, as in the case of CeCu(II)01. Comparing the theoretical amount of $H_2$ required for complete reduction in CuO in CeCu(II)05, 836 μmol/g, with actual amount, about 500 μmol $H_2$/g was consumed to reduce the $CeO_2$ support. This value was approximately similar to the amount assigned to ceria reduction in the CeCu(II)01 sample.

The total $H_2$ consumption during TPR of the CeCu(II)09 material was 1890 μmol $H_2$/g, and the reduction profile was similar to CeCu(II)05 sample, with a sharp peak at lower temperature, 76 °C, and a broader one at higher temperature, 128 °C. There was also an additional peak at 140 °C. Theoretically, 1454 μmol $H_2$/g was needed for complete CuO reduction in the copper in CeCu(II)09, and thus, about 440 μmol $H_2$/g was associated with reduction in the ceria support. Comparing CeCu(II)05, CeCu(II)09, and as suggested by Ayastuy et al. [61], it was hypothesized that the peak at 76 °C was related to reduction in highly dispersed CuO species not in strong contact with $CeO_2$, and the peaks at 128 °C might be related to simultaneous reduction in ceria and CuO species in direct contact with $CeO_2$. The peak at 140 °C is suggested to be associated with reduction in larger domains of crystalline/bulk CuO species. In all three cases, only 16–18% of the total $CeO_2$ was reduced. The collected TPR data coupled with PXRD data demonstrate that the CuO domains in the three supported samples are clearly different, being highly dispersed and non-crystalline in the low loading sample, and with the highest loading sample having some larger, crystalline CuO domains, some of which may be unsupported.

### 3.2. Catalytic reactivity

The oxidative coupling of benzylamine to form N-benzylidenebenzylamine in DMSO, Scheme 1, was evaluated over the series of

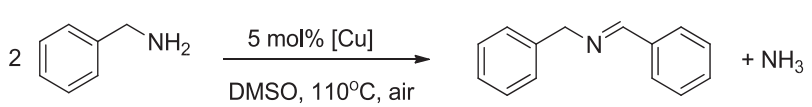


**Scheme 1.** Oxidative coupling of benzylamine to N-benzylidenebenzylamine.

copper oxide–ceria catalysts along with $CeO_2$ and copper(II) oxide as controls. As this catalytic conversion was discovered serendipitously while using dimethylsulfoxide (DMSO) as the solvent for another reaction, we continued to work with DMSO as the main solvent. Other solvents, such as toluene, were tried, but these solvents were found to be far less effective, likely due to their poor ability to solubilize copper (vide infra). The initial rate with toluene was one-third the initial rate with DMSO. Also, after 24 h, the product yield with toluene was one-third that using DMSO.

Fig. 1 shows the kinetic behavior of the benzylamine oxidative coupling reaction using CeCu(II)09 as the catalyst. After an induction period of 8 h, with an initial benzylamine conversion rate of 0.36 mmol/gcat h (3.85 mmol/gCu h or 3.39 μmol/$m^2$ cat h), the rate increased to 2.41 mmol/gcat h (26.1 mmol/gCu h or 22.9 μmol/$m^2$ cat h), and 90% product yield was obtained after 22 h. The product yield decreased after this point due to the decomposition of the product, N-benzylidenebenzylamine, to benzaldehyde, as verified by GC–MS analysis. The formation of benzaldehyde at extended reaction times was promoted by the presence of $H_2O$ produced from the dehydrogenation of benzylamine to benzylimine, Scheme 2. This was verified by running a reaction under the same conditions, starting with N-benzylidenebenzylamine and 1 equivalent $H_2O$. It was found that N-benzylidenebenzylamine decomposed linearly at a rate of 0.055 mmol/gcat h (0.60 mmol/gCu h)(0.524 μmol/$m^2$ h), with benzaldehyde being formed at a rate of 0.105 mmol/gcat h (1.14 mmol/gCu h)(1.0 μmol/$m^2$ h), which was stoichiometrically correct.

Given the complex shape of the kinetic profile for the CeCu(II)09 catalyst, the ceria support, unsupported CuO nanoparticles, and a physical mixture of the two oxides were evaluated in an attempt to gain further insight into the reactivity. Fig. 1 shows that the $CeO_2$ alone had moderate activity for the amine oxidation. A maximum yield of 41% was reached after 48 h. The shape of the kinetic profile was similar to that of the CeCu(II)09 catalyst, but as noted in Table 3, the rates in each stage were lower, and the induction period was somewhat prolonged. When using unsupported

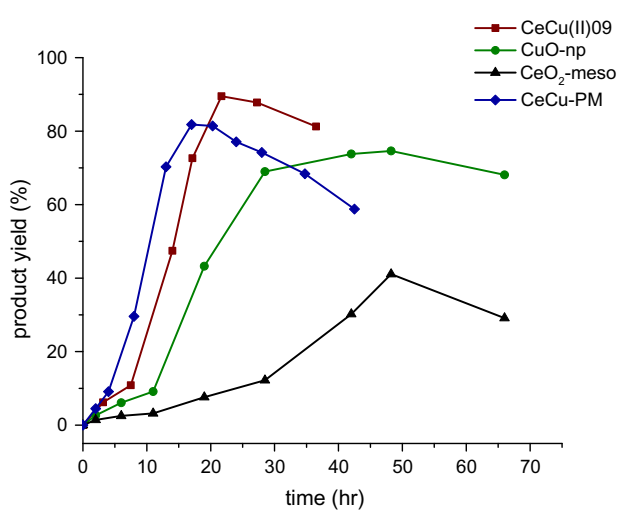


**Fig. 1.** Kinetic profiles for the oxidative coupling of benzylamine using the bare ceria support, unsupported CuO nanoparticles, a physical mixture of CuO nanoparticles and ceria, and the CeCu(II)09 material, as catalysts. Conditions: benzylamine (3 mmol), catalyst (5 mol% Cu), DMSO (3 ml), 110 °C, air.

**Table 3**
Rates of reaction over the various catalysts.[a]

| Catalyst | CeCu(II)09 | $CeO_2$ | CuO | CeCu-PM |
|---|---|---|---|---|
| *Initial amine conversion rate (in first 2 h)* | | | | |
| mmol/gcat h | 0.36 | 0.29 | 2.97 | 0.64 |
| mmol/gCu h | 3.85 | N/A | 3.71 | 7.08 |
| μmol/$m^2$ h | 3.39 | 1.38 | 247.2 | N/A |
| mmol/gCe h | 0.50 | 0.36 | N/A | 0.86 |
| *Highest observed amine conversion rate* | | | | |
| mmol/gcat h | 2.41 | 0.58 | 10.7 | 2.37 |
| mmol/gCu h | 26.1 | N/A | 13.3 | 26.4 |
| μmol/$m^2$ h | 22.9 | 2.74 | 888.4 | N/A |
| mmol/gCe h | 3.35 | 0.72 | N/A | 3.20 |

[a] Copper loading in case of CeCu(II)09, CuO, and CeCu-PM is 0.05 mole per mole of reactant. Cerium loading in case of $CeO_2$, CeCu(II)09, and CeCu-PM is 0.18 mole per mole reactant.

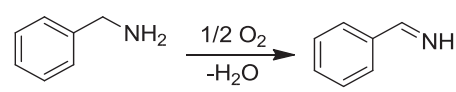


**Scheme 3.** Oxidative dehydrogenation of benzylamine to benzylimine.

CuO nanoparticles as the catalyst (referred to as CuO), an induction period of 11 h was observed, after which a maximum product yield of 75% was reached after 48 h. Interestingly, when a physical mixture of CuO and $CeO_2$ (referred to as CeCu-PM) was used as a catalyst, the initial rate was significantly higher than those of the individual oxides, with a significantly reduced induction period. After the first 4 h, the rate of reaction was almost the same as that of CeCu(II)09, after its induction period, as well as that of ceria-free CuO in its first 8 h, after its induction period. A maximum product yield of 82% was reached in 17 h. The initial and maximum observed rates in each case are given in Table 3. It is also important to note that the formation of benzaldehyde at extended reaction times was mostly promoted by $CeO_2$, as the rate of product decomposition in the case of CuO was much less than the rates in the other three experiments that have $CeO_2$ in the catalytic system.

The shape of the kinetic profiles may be used to gain insights into the roles of the CuO and $CeO_2$ phases in the oxidative coupling reaction. The CuO catalyst had a longer induction period than the CeCu(II)09 catalyst, and the physical mixture of oxides (CeCu-PM) had a severely reduced induction period. Furthermore, the initial rate of the CeCu-PM catalyst was approximately the sum of the initial rates of individual oxide catalysts, CuO and $CeO_2$. The first step of this reaction is believed to be the dehydrogenation of benzylamine to benzylimine (Scheme 3) [18], and in this regard, it has been reported by Tamura [65] that the N—H group of amines adsorbs on $CeO_2$ via the surface Lewis acid sites ($Ce^{4+}$) of $CeO_2$ and the strongly basic oxygen atom adjacent to the $Ce^{4+}$ cation (Scheme S1), and this may play a role in activating the N—H group in benzylamine. However, ceria alone appears inefficient in catalyzing the overall reaction, as observed in Fig. 1, with it showing the slowest initial and maximum observed rates, Table 3. On the other hand, if one compares the copper-containing catalysts CeCu(II)09, CuO, and CeCu-PM and excludes the induction periods, it is apparent that all these catalysts have a similar rate of reaction. This observation suggests that CuO species are the main catalysts for the overall process, ultimately producing the final product,

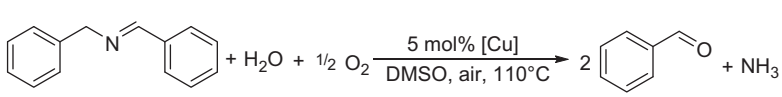


**Scheme 2.** N-Benzylidenebenzylamine decomposition to benzaldehyde.

N-benzylidenebenzylamine. The $CeO_2$, when present, may play a role of providing additional sites to promote the first step of the reaction.

The stability of the CeCu(II)09 catalyst was evaluated. After completing the reaction, the catalyst was recovered by centrifugation, washed with de-ionized water, and re-calcined at 500 °C. Elemental analyses of fresh and used catalysts show that the fresh catalyst had 9.2 wt% copper, with Cu/Ce molar ratio of 0.269 and that the re-calcined used catalyst had 8.6 wt% copper, with a 0.240 Cu/Ce molar ratio. Accordingly, 11% of copper was lost from the CeCu(II)09 catalyst after the first cycle.

Knowing that there was 11% copper leaching from the support in the first cycle, it became necessary to test the effect of that leached copper on the reactivity of the system. Running the same reaction under the same conditions (Scheme 1), in a second experiment, the catalyst was filtered off (hot filtration) when the product yield reached 30%. The solid-free reaction solution was allowed to continue to react, and the product yield was monitored. The reaction continued to proceed with a similar rate as before the filtration, suggesting that the leached copper species were largely responsible for the catalytic conversion when the reaction rate was highest, at moderate conversions. This supports the hypothesis that copper species were the main catalyst for the formation of the final product and suggests another cause, beyond generation of the initial imine intermediate, may contribute to the observed induction period, copper leaching.

To further clarify the role of ceria versus copper in this reaction and to test whether the induction period was related to copper leaching, an additional experiment was conducted. The reaction, shown in Scheme 1, was started with only $CeO_2$ as catalyst, and after 20 h, CuO was added to the reaction. As shown in Fig. 2, with $CeO_2$ alone, the rate of product formation was low, and once the CuO catalyst was added, the rate increased significantly, from 0.15 to 2.4 mmol/gcat h. This experiment further demonstrates that CuO species most efficiently promote the overall reaction and that the presence of $CeO_2$ primarily helps in shortening the induction period associated with the first step compared to using CuO alone.

To further resolve this issue, the same reaction starting with $CeO_2$ alone was run in parallel in three separate flasks for 5.5 h, after which solid CuO nanoparticles were added to two flasks (0.25 mol% and 1.25 mol%), and pre-dissolved, soluble CuO species (also at 0.25 mol%) were added to the third flask.[1] The initial kinetic profiles for these experiments are shown in Fig. 3. As shown in the figure, adding 1.25 mol% solid CuO nanoparticles increased the rate 5-fold compared to addition of 0.25 mol% solid CuO nanoparticles. On the other hand, when adding "soluble" and "solid" CuO nanoparticles at the same loading (0.25 mol%), there was almost no difference in the rate. Because pre-dissolved and solid CuO nanoparticles gave similar rates, one may view that these experiments support the hypothesis that the induction period might not be due to the time needed to solvate copper species, but instead may be due to the time needed to build sufficient amount of the intermediate, benzylimine, which is effectively promoted by both $CeO_2$ and copper species.

Nonetheless, additional tests were done to evaluate the relation between copper leaching and the production rate of the final coupled product, and the dissolved copper concentration was measured in another experiment (similar to that in Fig. 1 using

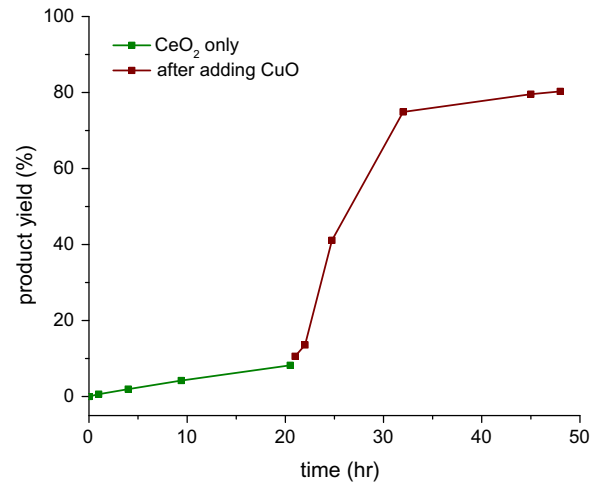


**Fig. 2.** Kinetic profiles for the oxidative coupling of benzylamine using the bare ceria support, followed by addition of unsupported CuO nanoparticles after 20 h. Reaction carried at 110 °C under air.

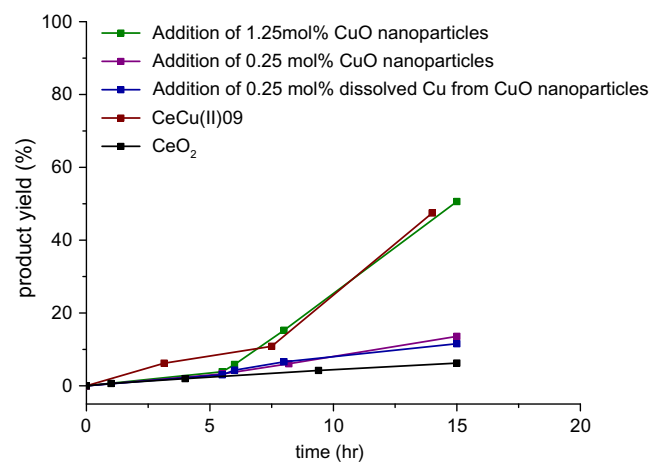


**Fig. 3.** Kinetic profiles for the oxidative coupling of benzylamine using the bare ceria support, followed by addition of "solid" and "soluble" copper species derived from CuO nanoparticles after 5.5 h. Reaction carried at 110 °C under air.

CeCu(II)09) as a function of time and related to product yield, as shown in Fig. 4. It is apparent that the rate increases in proportion to the amount of copper dissolved in the reaction mixture. In this experiment, samples were withdrawn at specified times, solid catalyst was removed by centrifugation, and the clear solution was sent to elemental analysis. As the copper concentration increased from 9 ppm to 95 ppm, the product yield increased accordingly from 8% to 85%. In contrast to the above paragraph, these experiments support the idea that CuO species dissolved in the reaction mixture are primarily responsible for the overall reaction, and contribute to the observed induction period.

Fig. 5 shows the kinetic profiles of supported catalysts with different copper loadings, CeCu(II)01, CeCu(II)05, and CeCu(II)09. It is clear that the low copper loading CeCu(II)01 catalyst had little or no induction period, and the overall kinetic profile appeared similar to reactions using pure ceria alone. Also, it can be observed that the maximum product yield increased with increasing copper loading, from 49% to 70% to 90% (note: reactions were conducted with fixed copper loading in the reactor and therefore with varied ceria content). This supports the hypothesis that a key role of $CeO_2$ may be reducing the induction period by catalyzing the first step of the reaction, as more $CeO_2$ is available in the case of CeCu(II)01

[1] Soluble CuO species were produced by stirring CuO nanoparticles at reaction temperature in DMSO for 15 h, then quickly centrifuging the mixture, and pipetting off the supernatant containing dissolved copper species while the solution was still warm. The residual CuO nanoparticles were dried and weighed, and this weight was used to estimate the amount of dissolved CuO species for comparison with solid addition.

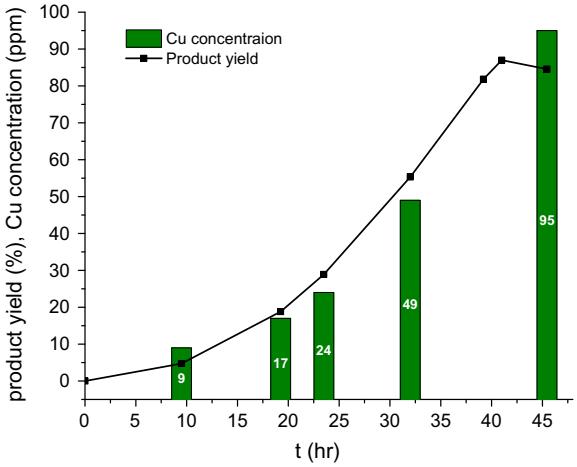


**Fig. 4.** Kinetic profiles for the oxidative coupling of benzylamine using CeCu(II)09 catalysts and the effect of Cu concentration in the solution on the product yield. Conditions: benzylamine (3 mmol), catalyst (5 mol% Cu), DMSO (3 ml), 110 °C, air.

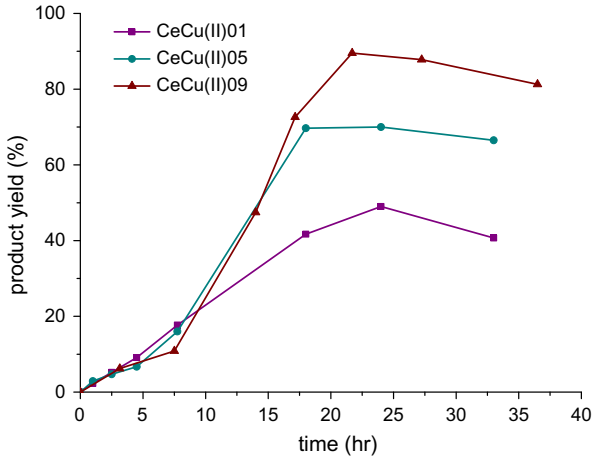


**Fig. 5.** Kinetic profiles for the oxidative coupling of benzylamine using ceria-supported catalysts with different Cu(II) loadings: CeCu(II)01, CeCu(II)05 and CeCu(II)09. Conditions: benzylamine (3 mmol), catalyst (5 mol% Cu), DMSO (3 ml), 110 °C, air.

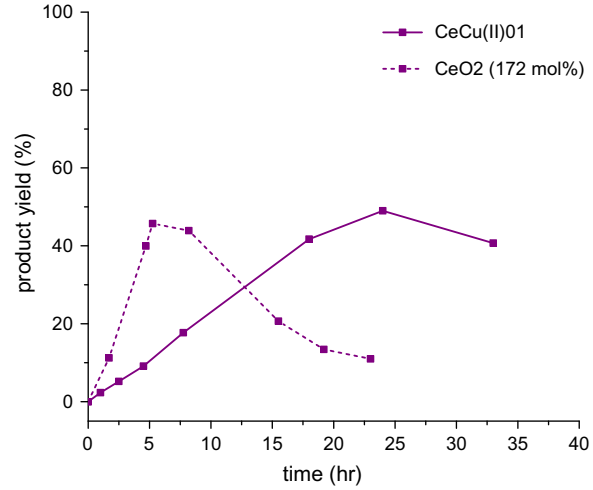


**Fig. 6.** Comparison between bare $CeO_2$ (172 mol%) and CeCu(II)01 as catalysts, and their effect on the kinetic profiles of the oxidative coupling of benzylamine. Reaction carried at 110 °C under air.

than in CeCu(II)05 and CeCu(II)09. An alternate explanation is that highly dispersed copper domains more slowly leach into solution, if one argues that copper dissolution is the main cause of the induction period. The reduction in product yield may be related to the amount of ceria in the reactor, since the ceria promotes product decomposition to benzaldehyde, as mentioned earlier.

To further understand the reduction in the induction period in the CeCu(II)01 experiment, the amount of $CeO_2$ in CeCu(II)01 was calculated, found to be 172 mol% based on reactant, and this amount of $CeO_2$ was used in a new experiment. In this experiment, shown in Fig. 6, the initial rate was almost four times the one with CeCu(II)01, and the product decomposition rate was about three times the rate observed CeCu(II)01. Keeping in mind that in the case of the $CeO_2$ experiment, though the $CeO_2$ loading was similar to the CeCu(II)01 catalyst, many more $CeO_2$ sites were available in this case, as the highly dispersed CuO species block access to $CeO_2$ sites. The observations support the hypotheses that $CeO_2$ promotes the decomposition of N-benzylidenebenzylamine to benzaldehyde and that the induction period can be reduced or eliminated (see Fig. 6) by adding $CeO_2$ to the reactor. This suggests that the initial slow step in the process, generating the imine intermediate, can be accelerated with $CeO_2$ domains, as shown in Scheme 3.

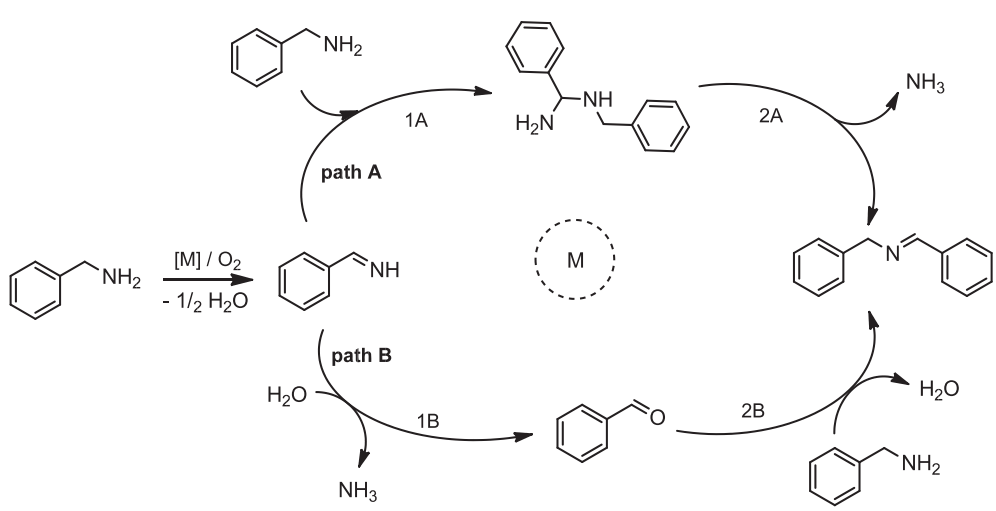


**Scheme 4.** Proposed reaction pathways for aerobic oxidation of benzylamine to benzylimine.

The collected data above argue for both copper and ceria species playing a role in the catalysis. The induction period is caused by multiple factors, an important one is copper dissolution, and a second one is the presence or absence of $CeO_2$, with $CeO_2$ shortening the induction period. Dissolved copper species appear to be the most effective catalysts for this reaction, and these species do not contribute appreciably to product decomposition, whereas $CeO_2$ domains lead to significant product decomposition and reduction in overall yield.

Scheme 4 depicts two hypothetical reaction pathways for the target aerobic oxidative benzylamine homocoupling reaction [18,66]. As noted above in Table 3, the CuO catalyst gave a much higher initial reaction rate (per gram catalyst) compared to $CeO_2$; however, addition of ceria to the CuO catalyst substantially shortened the induction period, as shown in Fig. 1. Since the first step of the coupling reaction, the dehydrogenation of the amine to an imine, produces water, and since $CeO_2$ has the ability to adsorb water, it was hypothesized that $CeO_2$ reduced the induction period not only by potentially activating the N—H group (kinetic effect), but also by adsorbing water (thermodynamic effect, shifting an equilibrium), and hence favoring the production of the intermediate benzylimine (Scheme 3). To test this hypothesis, $CeO_2$ was dried under vacuum at 200 °C overnight, and this dried $CeO_2$ was used in the same reaction. Fig. 7 compares the rates of this experiment with the experiment that used $CeO_2$ without drying. The data show dry $CeO_2$ was more active than the one stored under atmospheric conditions. The productivity of dry $CeO_2$ was almost double that of wet $CeO_2$ after 24 h of reaction. These results suggest that $CeO_2$ may promote this reaction by both activating the amine N—H and adsorbing the water produced from the first step of this oxidative coupling reaction (Scheme 3).

The reusability of the CeCu(II)09 catalyst in a subsequent catalytic reaction was evaluated. As mentioned earlier, after completing the reaction, the catalyst was recovered by centrifugation, washed with de-ionized water, and re-calcined at 500 °C, before use in a second cycle. Elemental analyses of fresh and used catalysts show that 11% of copper was lost from the CeCu(II)09 catalyst after the first cycle. Before use in a second cycle, this loss was taken into consideration, so that 5 mol% Cu was added to the reaction in both cases.

Fig. 8 shows the kinetic curve of the first cycle, using the fresh catalyst, and the second cycle, with the recovered, calcined catalyst. In the second cycle, the induction period decreased from 8 to 3 h, and the overall product yield was 90% of the first cycle. After the induction periods, the rates of reaction were almost the same

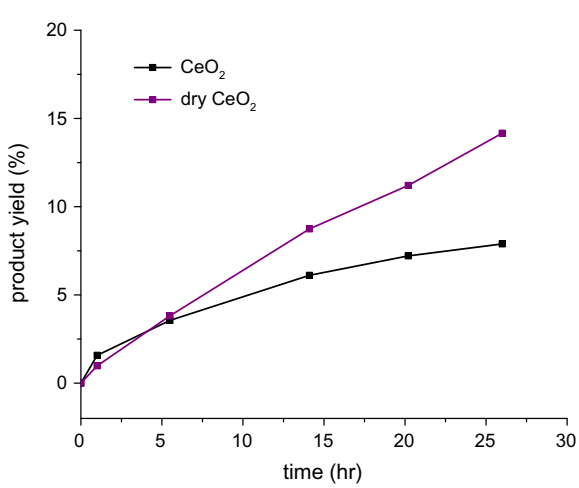


**Fig. 7.** Comparison between bare $CeO_2$ and dried, bare $CeO_2$ as catalysts, and their effect on the initial rate of amine oxidative coupling reaction. Reaction carried at 110 °C under air.

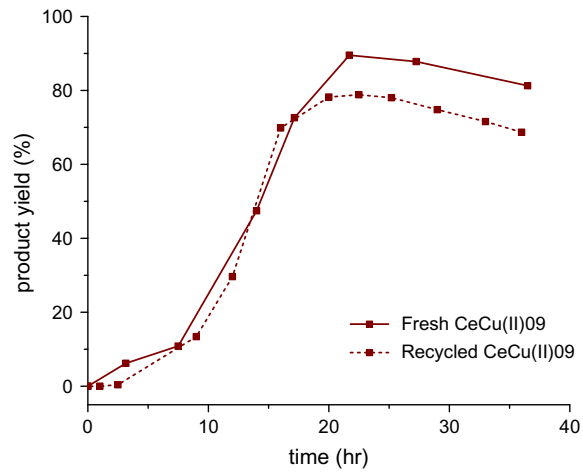


**Fig. 8.** Kinetic profiles for the oxidative coupling of benzylamine over two cycles using the CeCu(II)09 catalyst. Conditions: benzylamine (3 mmol), catalyst (5 mol% Cu), DMSO (3 ml), 110 °C, air.

in both cases, 1.54 ± 0.1 mmol/gcat h. Since the catalyst was re-calcined before recycling, carbon-desposition was excluded as the cause of the loss in yield. The reduction in the induction period may be associated with the presence of less CuO on the $CeO_2$ surface due to copper leaching, exposing more of the ceria surface, which is hypothesized to enhance the first dehydrogenative step of the reaction (see above). From PXRD (as shown in Fig. S1) using the Scherrer equation, the crystallite sizes of CuO and $CeO_2$ in the used catalyst were estimated to be 38 nm and 6.6 nm (4–5 μm particle size, Fig. S5), respectively. Comparing these values with those of the fresh catalyst, 28 nm and 6.1 nm, it seems that some copper agglomeration occurred after using the fresh catalyst. Given that in the work using different CuO loadings described above, the induction period was longest with the highest CuO loading and largest CuO domain size, the observation that the CuO domains were larger in the recycled catalyst, but a shorter induction period was observed suggests that the nature of the copper species did not have a dominant effect on the induction period. Rather, the induction period was likely shorter in the recycled catalysts due to greater exposed $CeO_2$ surface area. Also, as mentioned earlier, having more $CeO_2$ in the system means more decomposition of the final product to benzaldehyde, which may be another cause for the lower product yield.

### 3.3. Proposed reaction pathway

In the literature, two mechanisms have been proposed for the oxidation of primary amines to a dimeric imine product [18] as shown in Scheme 4. Both mechanisms proceed by way of an initial oxidative dehydrogenation of the amine to the imine intermediate, RCH=NH. For benzylamine, this intermediate is unstable and difficult to detect by routine spectroscopic techniques. In path A, the imine intermediate is then attacked by a second molecule of the primary amine, giving an aminal, which loses $NH_3$ to give the coupled imine product $RCH{=}NCH_2R$. In path B, the initially formed imine intermediate reacts with trace amounts of $H_2O$ to give the aldehyde RCH=O and $NH_3$, with the aldehyde subsequently reacting with a second molecule of the amine to give the imine product. The last step, 2B, is accomplished quickly under these reaction conditions; when benzylamine was added to benzaldehyde, with 5 mol% Cu from CeCu(II)09 in DMSO, the N-benzylidenebenzylamine yield was 95% immediately upon immersing the reaction flask in the 110 °C preheated oil bath.

To gain further insight into the reaction pathway, a control experiment was run under the exact same conditions (Scheme 1),

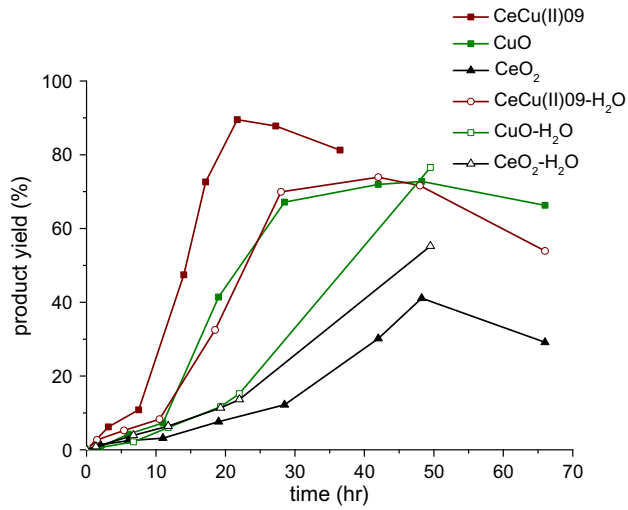


**Fig. 9.** Effect of adding 0.5 equivalents of water on the kinetic profiles of oxidative coupling of benzylamine using CuO, $CeO_2$, and CeCu(II)09 as catalysts. Reaction carried at 110 °C under air.

but without any catalyst. It was found that the initial rate was almost half of that observed in the experiment with $CeO_2$ alone. Other experiments were run under the same reaction conditions, but with the addition of 0.5 equivalents of water. Fig. 9 shows the kinetic profiles of the reactions with and without added water. Adding water to the CeCu(II)09 catalyst and the CuO catalyst significantly increased the induction periods in both cases, decreased the maximum observed rates by 50%, and decreased the maximum yield in the case of CeCu(II)09. On the contrary, adding $H_2O$ to $CeO_2$ alone increased its initial and maximum observed rates and led to higher maximum yield. These observations might suggest that CuO catalysis primarily follows path A, as added water shifts the formation of imine intermediate to the left and slows the overall reaction rate, while $CeO_2$ catalysis primarily follows path B, as excess $H_2O$ helps accelerate the hydrolysis of intermediate imine to the aldehyde, step 1B. This may be why CeCu(II)09 is more active than individual CuO and $CeO_2$, as it combines both pathways.

To further test this hypothesis, several other experiments were run, to study the relative rates of steps 1A and 1B using CuO and $CeO_2$ as catalysts. In these experiments, N-benzylidenemethylamine was used as a substrate because it is more stable than benzylimine and can be quantified using GC–FID. To study step 1A, benzylamine was added to 1 equivalent N-benzylidenemethylamine, with 5 mol% Cu from CuO in DMSO (Scheme S2). This reaction yielded 75% N-benzylidenebenzylamine immediately upon immersing the reaction flask in the 110 °C preheated oil bath. This observation strongly supports the hypothesis that copper mediated reactions proceed via path A. Running the same reaction, Scheme S2, with $CeO_2$ formed a minimal amount of desired product. To study step 1B, N-benzylidenemethylamine was added to 1 equivalent of $H_2O$, with 5 mol% Cu from CuO in DMSO. In this reaction, 12% benzaldehyde was formed in 12 h. When running the same reaction, 1B, using $CeO_2$ instead of CuO, 22% benzaldehyde was formed in 12 h. These data suggest that it is unlikely that CuO-based catalysts proceed via path B with significant rates under the conditions used here. In addition, when running the reaction starting with N-benzylmethylamine, it was noticed the rate of N-benzylidenemethylamine formation using CuO was double the rate observed using $CeO_2$, supporting the hypothesis mentioned earlier (in Section 3.2) that CuO domains may be the main catalysts for the overall process. It is also noteworthy that with $CeO_2$, more benzonitrile was formed than in the case with the CuO catalyst, which might explain the limited ability of $CeO_2$ to produce the desired final product, N-benzylidenebenzylamine, as intermediate was siphoned off into side-products.

After running this comprehensive set of experiments, it is proposed that the overall coupling reaction runs according to the following pathway: benzylamine is oxidatively dehydrogenated to the benzylimine intermediate by copper species, and this step is enhanced by the existence of $CeO_2$, which absorbs water molecules formed by this dehydrogenation, and thus shifts the reaction to the right. $CeO_2$ may participate, in parallel, in the catalytic dehydrogenation reaction. Once the benzylimine intermediate is formed, copper species catalyze the coupling with a second molecule of benzylamine, causing the fast formation of the final product, N-benzylidenebenzylamine, and the loss of $NH_3$ (path A). On the other hand, $CeO_2$ can competitively convert the benzylimine intermediate to benzaldehyde, at a slower rate, and once the benzaldehyde is formed, it spontaneously reacts with a second molecule of the benzylamine to give the final imine product, N-benzylidenebenzylamine (path B). Based on the reaction rates observed, this pathway is less important under the conditions used here.

## 4. Conclusions

Copper oxide supported on ceria (CuO—$CeO_2$) was shown to be an effective, somewhat stable, and recyclable catalyst for the direct synthesis of imines from amines under aerobic conditions. Copper(II) oxide and ceria alone also promoted the conversion, but not as efficiently as the combined catalyst. Varying the loading of the copper(II) oxide on the ceria support affected the overall product yield, as well as the induction period; catalysts with higher copper loading gave higher yield of N-benzylidenebenzylamine due to the higher rate of product formation over copper oxide domains and the reduced ceria content in the reactor, as the ceria promoted product decomposition. Leaching studies demonstrated that the majority of the copper catalysis occurred in solution.

A series of experiments demonstrated that ceria and copper domains promote the reaction primarily via two distinct pathways. Both pathways begin with an initial oxidative dehydrogenation of the amine to form an imine. Subsequently, copper(II) oxide domains appeared to primarily promote product formation via path A, involving the coupling of benzylimine with a second molecule of benzylamine, with liberation of ammonia. In contrast, ceria produced the N-benzylidenebenzylamine product more slowly, primarily via path B, involving hydrolysis of the benzylimine to form benzaldehyde, which was quickly coupled with benzylamine to form the N-benzylidenebenzylamine product.

This CuO—$CeO_2$ catalytic system has the advantages of being both easily separated from the reaction media and more active than unsupported CuO nanoparticles at similar copper loadings, because of the added efficiency of $CeO_2$ domains. However, the catalyst is not fully recyclable, as the copper catalysis occurs in solution, and thus the catalyst may only be reused to good effect until the copper reservoir is depleted.

## Acknowledgment

This work was supported by the American Chemical Society Petroleum Research Fund (ACS-PRF) through Contract 48034-AC1.

## Appendix A. Supplementary material

Supplementary data associated with this article can be found, in the online version, at http://dx.doi.org/10.1016/j.jcat.2013.01.027.

## References


[1] L. Blackburn, R.J.K. Taylor, Org. Lett. 3 (2001) 1637.
[2] D. Gnanamgari, E.L.O. Sauer, N.D. Schley, C. Butler, C.D. Incarvito, R.H. Crabtree, Organometallics 28 (2009) 321.
[3] H. Sun, F.Z. Su, J. Ni, Y. Cao, H.Y. He, K.N. Fan, Angew. Chem. Int. Edit. 48 (2009) 4390.
[4] S. Kegnaes, J. Mielby, U.V. Mentzel, C.H. Christensen, A. Riisager, Green Chem. 12 (2010) 1437.
[5] M.A. Esteruelas, N. Honczek, M. Olivan, E. Onate, M. Valencia, Organometallics 30 (2011) 2468.
[6] W. He, L.D. Wang, C.L. Sun, K.K. Wu, S.B. He, J.P. Chen, P. Wu, Z.K. Yu, Chem.-Eur. J. 17 (2011) 13308.
[7] L. Jiang, L.L. Jin, H.W. Tian, X.Q. Yuan, X.C. Yu, Q. Xu, Chem. Commun. 47 (2011) 10833.
[8] C. Xu, L.Y. Goh, S.A. Pullarkat, Organometallics 30 (2011) 6499.
[9] G.B. Chu, C.B. Li, Org. Biomol. Chem. 8 (2010) 4716.
[10] A. Dhakshinamoorthy, M. Alvaro, H. Garcia, Chemcatchem 2 (2010) 1438.
[11] Q.L. Yuan, X.T. Zhou, H.B. Ji, Catal. Commun. 12 (2010) 202.
[12] S. Furukawa, Y. Ohno, T. Shishido, K. Teramura, T. Tanaka, ACS Catal. 1 (2011) 1150.
[13] R.D. Patil, S. Adimurthy, Adv. Synth. Catal. 353 (2011) 1695.
[14] X.J. Lang, W.H. Ma, Y.B. Zhao, C.C. Chen, H.W. Ji, J.C. Zhao, Chem.-Eur. J. 18 (2012) 2624.
[15] K. Orito, T. Hatakeyama, M. Takeo, S. Uchiito, M. Tokuda, H. Suginome, Tetrahedron 54 (1998) 8403.
[16] T. Mukaiyama, A. Kawana, Y. Fukuda, J. Matsuo, Chem. Lett. (2001) 390.
[17] H. Choi, M.P. Doyle, Chem. Commun. (2007) 745.
[18] B.L. Zhu, M. Lazar, B.G. Trewyn, R.J. Angelici, J. Catal. 260 (2008) 1.
[19] G. Jiang, J. Chen, J.S. Huang, C.M. Che, Org. Lett. 11 (2009) 4568.
[20] M.H. So, Y.G. Liu, C.M. Ho, C.M. Che, Chem.-Asian J. 4 (2009) 1551.
[21] A. Prades, E. Peris, M. Albrecht, Organometallics 30 (2011) 1162.
[22] T. Hirao, M. Higuchi, Y. Ohshiro, I. Ikeda, Chem. Lett. (1993) 1889.
[23] K. Nakayama, M. Hamamoto, Y. Nishiyama, Y. Ishii, Chem. Lett. (1993) 1699.
[24] L. Aschwanden, B. Panella, P. Rossbach, B. Keller, A. Baiker, Chemcatchem 1 (2009) 111.
[25] L. Aschwanden, T. Mallat, F. Krumeich, A. Baiker, J. Mol. Catal. a – Chem. 309 (2009) 57.
[26] K.W. Chi, H.Y. Hwang, J.Y. Park, C.W. Lee, Synth. Met. 159 (2009) 26.
[27] Y. Perez, C. Aprile, A. Corma, H. Garcia, Catal. Lett. 134 (2010) 204.
[28] H.F. Guo, M. Kemell, A. Al-Hunaiti, S. Rautiainen, M. Leskela, T. Repo, Catal. Commun. 12 (2011) 1260.
[29] X.J. Lang, H.W. Ji, C.C. Chen, W.H. Ma, J.C. Zhao, Angew. Chem. Int. Edit. 50 (2011) 3934.
[30] M.T. Schümperli, C. Hammond, I. Hermans, ACS Catal. 2 (2012) 1108.
[31] S. Minakata, Y. Ohshima, A. Takemiya, I. Ryu, M. Komatsu, Y. Ohshiro, Chem. Lett. (1997) 311.
[32] A. Grirrane, A. Corma, H. Garcia, J. Catal. 264 (2009) 138.
[33] S. Kodama, J. Yoshida, A. Nomoto, Y. Ueta, S. Yano, M. Ueshima, A. Ogawa, Tetrahedron Lett. 51 (2010) 2450.
[34] S.-i. Naya, K. Kimura, H. Tada, ACS Catal. 3 (2013) 10.
[35] P. Bera, S.T. Aruna, K.C. Patil, M.S. Hegde, J. Catal. 186 (1999) 36.
[36] Y.H. Hu, L. Dong, J. Wang, W.P. Ding, Y. Chen, J. Mol. Catal. a – Chem. 162 (2000) 307.
[37] N.A.S. Amin, E.F. Tan, Z.A. Manan, Appl. Catal. B – Environ. 43 (2003) 57.
[38] X.Y. Jiang, L.P. Lou, Y.X. Chen, X.M. Zheng, J. Mol. Catal. a – Chem. 197 (2003) 193.
[39] G.R. Rao, H.R. Sahu, B.G. Mishra, Colloids Surf. a – Physicochem. Eng. Aspects 220 (2003) 261.
[40] M. Khristova, B. Ivanov, I. Spassova, T. Spassov, Catal. Lett. 119 (2007) 79.
[41] C.C. Pantazis, D.E. Petrakis, P.J. Pomonis, Appl. Catal. B – Environ. 77 (2007) 66.
[42] J. Beckers, G. Rothenberg, Dalton Trans. (2008) 6573.
[43] L.J. Liu, B. Liu, L.H. Dong, J. Zhu, H.Q. Wan, K.Q. Sun, B. Zhao, H.Y. Zhu, L. Dong, Y. Chen, Appl. Catal. B – Environ. 90 (2009) 578.
[44] J.F. Chen, Y.Y. Zhan, J.J. Zhu, C.Q. Chen, X.Y. Lin, Q. Zheng, Appl. Catal. a – Gen. 377 (2010) 121.
[45] L.J. Liu, Z.J. Yao, Y. Deng, F. Gao, B. Liu, L. Dong, Chemcatchem 3 (2011) 978.
[46] A. Martinez-Arias, A.B. Hungria, A. Iglesias-Juez, M. Fernandez-Garcia, J.A. Anderson, J.C. Conesa, G. Munuera, J. Soria, Catal. Today 180 (2012) 81.
[47] M.F. Luo, J.M. Ma, J.Q. Lu, Y.P. Song, Y.J. Wang, J. Catal. 246 (2007) 52.
[48] M.H. Lu, M.S. Li, Y.H. Shan, K. Seshan, L. Lefferts, Chin. J. Chem. 26 (2008) 1035.
[49] R. Zhang, T. Haddadin, D.P. Rubiano, H. Nair, C.S. Polster, C.D. Baertsch, ACS Catal. 1 (2011) 519.
[50] P. Djinovic, J. Batista, A. Pintar, Catal. Today 147 (2009) S191.
[51] R.K. Pati, I.C. Lee, S.C. Hou, O. Akhuemonkhan, K.J. Gaskell, Q. Wang, A.I. Frenkel, D. Chu, L.G. Salamanca-Riba, S.H. Ehrman, ACS Appl. Mater. Interf. 1 (2009) 2624.
[52] P. Gawade, B. Mirkelamoglu, U.S. Ozkan, J. Phys. Chem. C 114 (2010) 18173.
[53] L. Li, L. Song, H.D. Wang, C.Q. Chen, Y.S. She, Y.Y. Zhan, X.Y. Lin, Q. Zheng, Int. J. Hydrogen Energ 36 (2011) 8839.
[54] R. Si, J. Raitano, N. Yi, L.H. Zhang, S.W. Chan, M. Flytzani-Stephanopoulos, Catal. Today 180 (2012) 68.
[55] J.K. Zhu, Q.M. Gao, Z. Chen, Appl. Catal. B – Environ. 81 (2008) 236.
[56] L.M. Wan, X.Z. Cui, H.R. Chen, J.L. Shi, Mater. Lett. 64 (2010) 1379.
[57] W.W. Lukens, P. Schmidt-Winkel, D.Y. Zhao, J.L. Feng, G.D. Stucky, Langmuir 15 (1999) 5403.
[58] X. Tang, B. Zhang, Y. Li, Y. Xu, Q. Xin, W. Shen, Catal. Today 93–95 (2004) 191.
[59] H. Zou, X. Dong, W. Lin, Appl. Surf. Sci. 253 (2006) 2893.
[60] J.L. Ayastuy, N.K. Gamboa, M.P. González-Marcos, M.A. Gutiérrez-Ortiz, Chem. Eng. J. 171 (2011) 224.
[61] J.L. Ayastuy, A. Gurbani, M.P. Gonzalez-Marcos, M.A. Gutierrez-Ortiz, Int. J. Hydrogen Energy 35 (2010) 1232.
[62] G. Avgouropoulos, T. Ioannides, Appl. Catal. A: Gen. 244 (2003) 155.
[63] P. Zhu, J. Li, S. Zuo, R. Zhou, Appl. Surf. Sci. 255 (2008) 2903.
[64] A. Gómez-Cortés, Y. Márquez, J. Arenas-Alatorre, G. Díaz, Catal. Today 133–135 (2008) 743.
[65] M. Tamura, T. Tonomura, K. Shimizu, A. Satsuma, Green Chem. 14 (2012) 717.
[66] M.K. Patil, M. Keller, B.M. Reddy, P. Pale, J. Sommer, Eur. J. Org. Chem. (2008) 4440.